Conclusions

Transport of O_2 by rHSA−heme complexes could be of great clinical importance, not only as a blood alternative but also as an O_2-providing therapeutic fluid. Such a synthetic compound has the potential advantage of not having to be matched to the recipient's blood type; moreover, it could be prepared in controlled facilities without viral contamination.

We have previously demonstrated that rHSA−heme complexes can be engineered to bind O_2 reversibly;[11] however, these complexes did not display optimal O_2 binding affinities. By use of structure-based mutagenesis of HSA combined with chemical modification of the synthetic iron−porphyrin, we have attempted to modify the heme pocket architecture so as to refine the O_2 binding properties of rHSA−heme complexes. By focusing on modifications on the distal side of the heme binding pocket in rHSA, we have successfully engineered distinct rHSA(triple mutant)−heme complexes with a broad range of O_2 binding affinities. Schematic illustrations of the engineered distal amino acids in the heme pocket of the different rHSA mutants are shown in Figure 10. These include mutants such as rHSA(HL/L185N) with affinities that mimic the high affinity of Hb(α) ($P_{1/2}^{O_2}$ 0.24 Torr) and others [e.g., rHSA(HL/R186L)] with affinities similar to that of human RBC ($P_{1/2}^{O_2}$ 8 Torr).

The highest affinity mutants rHSA(HL/L185N) and rHSA-(HF/L185N) both contain Asn-185, which has a short amide side chain that significantly enhances the O_2 binding affinity, particularly when the neighboring amino acid is Leu-161. The N−H bond of the Asn-185 may face the terminal oxygen atom of the Fe−O_2 moiety, providing an amide dipole that stabilizes the O_2 binding to the heme. This interpretation is consistent with the findings of Chang et al.,[36] who first demonstrated that the dipole−dipole interaction between the Fe−O_2 and amide group can produce kinetic and thermodynamic control of the dioxygenation of the model hemes. In contrast, introduction of the larger Gln and His side chains at position 185 partly provided a six-coordinate heme character and therefore did not stabilize O_2 binding.

In a different approach, substitution of the polar Arg-186 at the entrance of the heme pocket with Leu or Phe caused a useful reduction in the O_2 binding affinity, yielding $P_{1/2}^{O_2}$ values that are very close to that of the human RBC and therefore well adapted for O_2 transport in vivo (Table 2). The impact of these substitutions may be due to their interaction with the adjacent residue, L185, which results in enhanced access to the O_2 binding site.

(36) Chang, C. K.; Ward, B.; Young, R.; Kondylis, M. P. *J. Macromol. Sci., Chem.* **1988**, *A25*, 1307−1326.

Other mutations were deleterious to O_2 binding but nevertheless produced complexes that might have other uses. For example, rHSA(HF/R186H)−heme formed a typical bis-histidyl Fe^{3+} or Fe^{2+} complex. In the circulation, free hemin is known to participate in the Fenton reaction to produce the highly toxic hydroxyl radical. However, it is sequestered by Hpx, in which the bis-histidyl coordination tightly fixes the hemin with the highest binding affinity of any known protein.[1,2] In the same manner, rHSA(HF/R186H) has a bis-histidine clamp for hemin and might conceivably be exploited as an antioxidant reagent to protect the body from oxidative damage after blood heme overload.

On the other hand, it would be of great importance to study the NO binding property of rHSA(mutant)−heme for practical medical applications. Some of the Hb-based blood substitutes leak through the vascular endothelium and capture the endothelial-derived relaxing factor, NO, that elicits an acute increase in blood pressure by vasoconstriction.[37] Our rHSA(mutant)−heme would bind NO in the same way as Hb, but it would not induce such hypertension, because the albumin carrier has low permeability through the muscle capillary pore.[38]

Ultimately, to fully understand the structural basis of the effects of the various mutations on O_2 binding, it will be necessary to examine the structural details of the heme binding pocket. Crystal structural analysis of the rHSA(mutant)−heme complexes is now underway. Structural information should enhance our ability to design mutations that will further optimize the O_2 binding properties of these complexes.

Acknowledgment. This work was supported by PRESTO "Control of Structure and Functions", JST, Grant-in-Aid for Scientific Research (16350093) from JSPS, and by Health Science Research Grants (Regulatory Science) from MHLW Japan. The work at Imperial College London was partially carried out as the Japan−U.K. Research Cooperative Program (Joint Project) of JSPS.

Supporting Information Available: UV−Visible absorption and MCD spectra of rHSA(HL/L185Q)−heme, absorption decay of O_2 rebinding to rHSA(HL/L185N)−heme after laser flash photolysis, and MCD spectra of rHSA(HL/R186F)−heme complex. This material is available free of charge via the Internet at http://pubs.acs.org.

JA074179Q

(37) Squires, J. E. *Science* **2002**, *295*, 1002−1005.
(38) Tsuchida, E.; Komatsu, T.; Matsukawa, Y.; Nakagawa, A.; Sakai, H.; Kobayashi, K.; Suematsu, M. *J. Biomed. Mater. Res.* **2003**, *64A*, 257−261.

Heme Pocket Architecture in Human Serum Albumin: Regulation of O_2 Binding Affinity of a Prosthetic Heme Group by Site-Directed Mutagenesis

Teruyuki Komatsu,[1,2,*] *Akito Nakagawa*[1] *and Eishun Tsuchida*[1,*]

[1] Research Institute for Science and Engineering, Waseda University, 3-4-1 Okubo, Shinjuku-ku, Tokyo 169-8555, Japan, Fax: (+81) 3-3205-4740; E-mail: teruyuki@waseda.jp

[2] PRESTO, Japan Science and Technology Agency (JST).

Summary: We present the O_2 binding properties of recombinant human serum albumin (rHSA) mutants complexed with an iron(II) protoporphyrin IX as a prosthetic heme group. Iron(III) protoporphyrin IX (hemin) is bound within subdomain IB of HSA with weak axial coordination by Tyr-161. In order to confer O_2 binding capability to this naturally occurring hemoprotein: (i) a proximal histidine was introduced into position Ile-142; and (ii) the coordinated Tyr-161 was replaced with hydrophobic Leu using site-directed mutagenesis. It provided a recombinant HSA double-mutant [rHSA(I142H/Y161L) = rHSA(HL)]. The rHSA(HL)–heme formed a ferrous five-coordinate high-spin complex with axial ligation of His-142 under an Ar atmosphere. This artificial hemoprotein binds O_2 at room temperature. Laser flash photolysis experiments demonstrated that O_2 rebinidng to rHSA(HL)–heme displays monophasic kinetics, whereas the CO recombination process obeyed a double-exponential pattern. This might be attributable to the two different geometries of the axial imidazole coordination arising from the two orientations of the porphyrin plane in the heme pocket. The O_2 binding affinity of rHSA(HL)–heme was considerably lower than those of R-state hemoglobin (Hb) and myoglobin (Mb), principally because of the high O_2 dissociation rate constant. The third mutations have been introduced into the distal side of the heme (at position Leu-185 or Arg-186) to increase the O_2 binidng affinity. The rHSA(HL/L185N)–heme showed high O_2 binding affinity ($P_{1/2}^{O_2}$: 1 Torr), which is 18-fold greater than that of the original double mutant rHSA(HL)–heme and which is rather close to those of Hb (R-state) and Mb. Furthermore, replacement of polar Arg-186 with Leu or Phe adjusted the O_2 binding affinity ($P_{1/2}^{O_2}$) to 10 Torr, which is almost equivalent to value for human red blood cells.

Keywords: biomimetics; heme; human seruma albumin; O_2 binidng; proteins

Introduction

Human serum albumin (HSA), the most abundant plasma protein (4–5 g/dl) in our circulatory system, is characterized by its remarkable ability to bind widely various endogenous and exogenous compounds[1] such as fatty acids, bilirubin, bile acids, thyroxine,[2,3] and a wide range of drugs.[4] Hemin [iron(III) protoporphyrin IX] released from methemoglobin is also captured by HSA with a high binding constant ($K \approx 10^8$ M^{-1}).[5] This strong affinity of HSA for hemin has stimulated efforts to develop albumin as an artificial hemoprotein which can mimic the O_2 binding ability of hemoglobin (Hb) and myoglobin (Mb).[6,7] HSA consists of a helical monomer of 66.5 kDa containing three homologous domains (I–III), each of which comprises of A and B subdomains.[8] Crystallographic studies have revealed that hemin is bound within a narrow D-shaped hydrophobic cavity in subdomain IB with axial coordination of Tyr-161 to the central ferric ion and electrostatic interactions between the porphyrin propionates and a triad of basic amino acid residues (Arg-114, His-146 and Lys-190) (Figure 1).[9,10] In terms of the general hydrophobicity of this α-helical heme pocket, the subdomain IB of HSA potentially has similar features to the heme binding site of Hb or Mb. However, if one reduces the HSA–hemin to obtain the ferrous complex, it is rapidly oxidized by O_2, even at low temperature, because HSA lacks the proximal histidine that enables the prosthetic heme group to bind O_2 and serves to regulate the O_2 binding affinity (Figure 1). In order to confer the O_2 binding capability to this

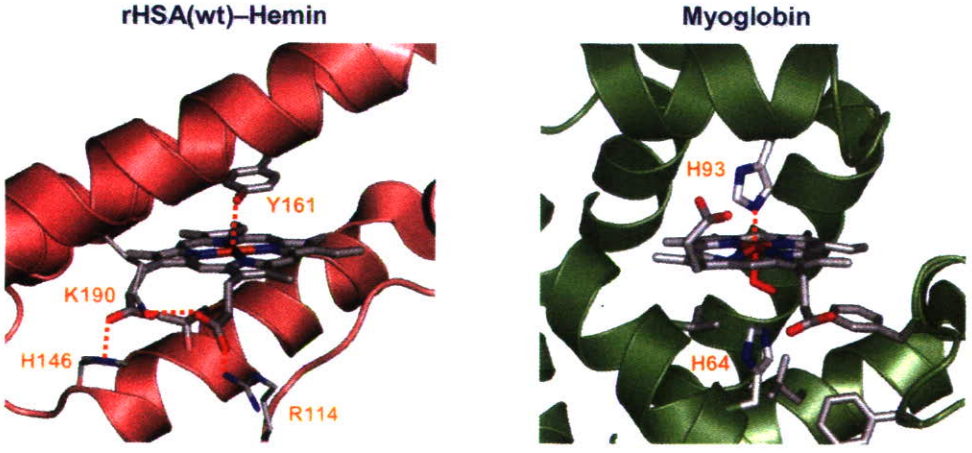

Figure 1. Heme pocket structure in subdomain IB of HSA (left; 1O9X from ref. 9) and heme pocket structure of Mb (1MBO).

naturally occurring hemoprotein, we have introduced a proximal histidine into the heme binding site of HSA by site-directed mutagenesis; it would provide axial coordination to the central ferrous ion of the heme and thereby promote O_2 binding.[11] Moreover, to modulate its O_2 binding affinity, we have added further modification to the distal side of the heme. The O_2 binding properties of several rHSA(mutant)–heme complexes have been characterized kinetically and compared to those of the natural Hb, Mb, and red blood cells (RBC). We have shown that our mutagenesis approach can create a new class of albumin-based artificial hemoprotein which would serve as an O_2 carrier.

Results and Discussion

Double-mutations to confer the O_2 binding capability

The detailed structure of the heme binding site in HSA revealed by crystallographic studies allows the design of mutagenesis experiments to construct a tailor-made heme pocket for O_2 binding.[9,10] In fact, Tyr-161 was the first candidate to introduce a proximal histidine (Figure 1). However, the Y161H mutation was not done because our simulation indicated that the distance from His-161 to the central Fe would be too great (4.0 Å). Instead, modeling experiments suggested that the favorable positions for the axial imidazole insertion would be Ile-142 (Figure 2a). The N(histidine)–Fe distance was estimated as 2.31 Å for H142 (compared to 2.18 Å for Mb). We therefore designed a recombinant HSA (rHSA) double-mutant I142H/Y161L [= rHSA(HL)].

The specific mutations were introduced into the HSA coding region in the plasmid vector (pHIL-D2 HSA) using the QuikChange mutagenesis kit (Stratagene), and clones were expressed in the yeast *Pichia pastoris* (Invitrogen Corp.). The rHSA–hemin complexes were prepared fundamentally according to our previously reported procedures.[9,11]

The MCD spectra of the rHSA(HL)–hemin showed S-shaped patterns in the Soret band region, which resembled that of ferric Mb.[12] One water molecule is known to coordinate axially to the sixth position of the central ferric ion of the hemin in metMb. Our MCD result suggests that the rHSA(HL)–hemin is also in a ferric high-spin complex, having a water molecule as the sixth ligand.

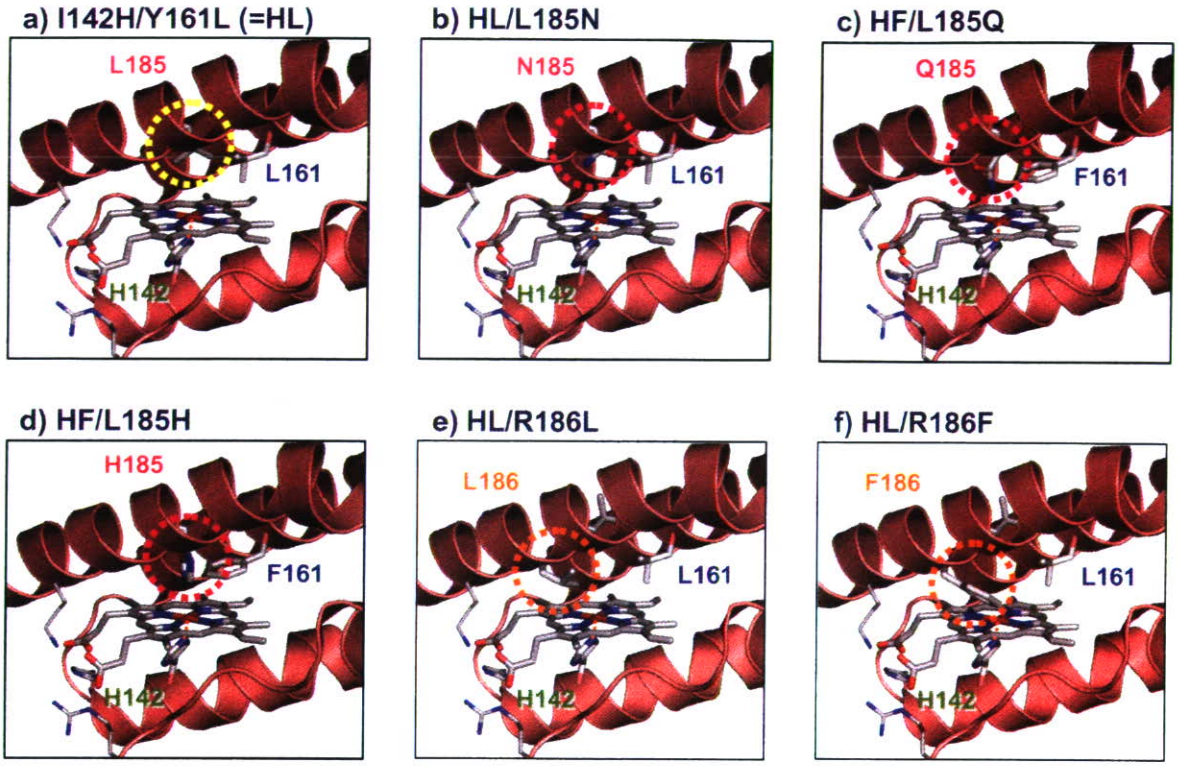

Figure 2. Structural models of the heme pocket in rHSA(mutant)–heme complexes.

O_2 Binding affinity of rHSA(HL)–heme

The rHSA(HL)–hemin was reduced to a ferrous complex by adding a small molar excess of aqueous sodium dithionate under an Ar atmosphere. A single broad absorption band (λ_{max}: 559 nm) in the visible region of rHSA(HL)–heme resembled that observed for deoxy Mb[13] or the chelated protoheme in DMF,[14] indicating the formation of a five-coordinate high-spin complex. The heme therefore appears to be accommodated in the mutated heme pocket with an axial coordination involving His-142. Upon exposure of the rHSA(HL)–heme solution to O_2, the UV-vis absorption immediately changed to that of the O_2 adduct complex at 0–25 °C.[13,14] After introduction of CO gas, the hemoprotein produced a stable carbonyl complex.

Laser flash photolysis experiments were carried out to evaluate the kinetics of the O_2 binding to the rHSA(HL)–heme.[11,15,16] The absorbance decay accompanying the O_2 recombination to rHSA(HL)–heme was composed of single-exponential. On the other hand, the rebinding of CO followed biphasic decay, which is normally not observed in Mb. Results

of numerous investigations of synthetic model hemes have shown that a bending strain in the proximal base coordination to the central ferrous ion, the "proximal-side steric effect", can decrease the association rate for CO without greatly altering the kinetics of O_2 association.[15,16] Therefore, a possible explanation is that there are two different geometries of the axial histidine (His-142) coordination to the central ferrous ion of the heme in rHSA(HL), each one accounting for the biphasic kinetics of CO rebinding.

By analyzing the CO/O_2 competitive binding following laser flash photolysis,[15,16] we obtained the association rate constants for O_2 ($k_{on}^{O_2}$) and the O_2 binding affinities [$P_{1/2}^{O_2} = (K^{O_2})^{-1}$] for rHSA(HL)–heme (Table 1).[11] The faster phase, defined as species I, and the slower phase, defined as species II, yielded two different O_2 binding affinities. In species I, the proximal His might coordinate to the central ferrous ion without strain, whereas in species II, the ligation might involve some distortion, resulting in weaker O_2 binding (Figure 3).

Table 1. O_2 binding parameters of rHSA(mutant)–heme complexes.[a]

Hemoproteins	$10^{-6}\ k_{on}^{O_2}$ ($M^{-1}s^{-1}$)	$10^{-3}\ k_{off}^{O_2}$ (s^{-1})		$P_{1/2}^{O_2}$ (Torr)	
		I	II	I	II
rHSA(HL)–Heme	7.5	0.22	1.70	18	134
rHSA(HL/L185N)–Heme	14	0.02	0.29	1	14
rHSA(HL/R186L)–Heme	25	0.41	8.59	10	209
rHSA(HL/R186F)–Heme	21	0.29	7.01	9	203
Hb(α) (R-state)[b]	33[c]	0.013[d]		0.24	
Mb[e]	14	0.012		0.51	
RBC[f]				8	

[a] In 50 mM potassium phosphate buffered Solution (pH 7.0) at 22°C. I or II indicates species I or II.
[b] Human Hb α-subunit.
[c] In 0.1 M phosphate buffer (pH 7.0, 21.5°C); ref 17.
[d] In 10 mM phosphate buffer (pH 7.0, 20°C); ref 18.
[e] Sperm whale Mb. In 0.1 M potassium phosphate buffer (pH 7.0, 20°C); ref 19.
[f] Human red cell suspension. In isotonic buffer (pH 7.4, 20°C); ref 23.

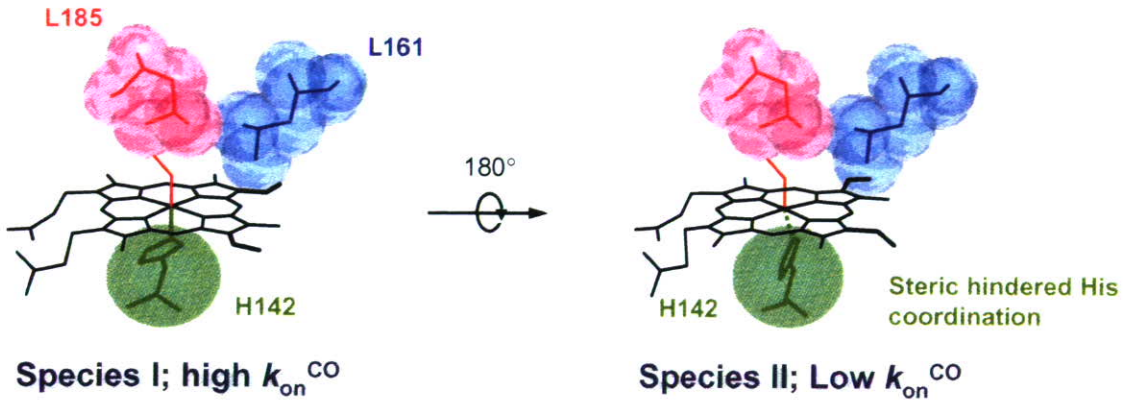

Figure 3. Structural models of heme-O_2 site of rHSA(HL)–heme complex.

The $P_{1/2}^{O_2}$ value of rHSA(HL)–heme was determined to be 18 Torr (species I), which was 35–75-fold higher (O_2 binding affinity is lower) than those of Hbα (R-state) and Mb.[17–19] This low affinity for O_2 was kinetically attributable to a 17–18-fold increases in the O_2 dissociation rate constants. The O_2 binding affinity should be adjusted to similar values for Hb and human RBC to develop this artificial hemoprotein as a blood substitute.

Introduction of Distal Base into the 185 Position

The His-64 in Hb and Mb on the distal side of the heme plays an important role for tuning their ligand affinities. A neutron diffraction study of MbO_2 showed that the N–H bond of the distal His-64 is restrained from optimal alignment for strong H–bonding with the coordinated O_2.[20] Olson and co-workers reported that the substitution of Gly for His-64 in Mb and Hb(α) caused a marked decrease in the O_2 binding affinity.[21] In view of these investigations, we reasoned that systematic variation of the steric hindrance and local polarity of the heme pocket in subdomain IB of HSA would allow modulation of the O_2 binding affinity. One approach to enhancing the O_2 binding affinity of rHSA–heme would be to introduce a basic amino acid into an appropriate position on the distal side of the heme. Our modeling results showed that the favorable position for the distal base insertion was Leu-185. Consequently, we replaced Leu-185 in rHSA(HL) [or rHSA(I142H/Y161F) [= rHSA(HF)]] with Asn, Gln, and His using site-directed mutagenesis (Figure 2b–2d).[22]

The rHSA(HL/L185N)–heme under Ar atmosphere showed a visible absorption band at 559 nm with a small shoulder at 530 nm, which was similar to the spectrum observed for rHSA(HL)–heme,[11] deoxy Mb,[13] and chelated protoheme.[14] The spectral pattern clearly indicated the formation of a five-coordinate high-spin complex. On the contrary, in the spectra of rHSA(HF/L185Q)–heme and rHSA(HF/L185H)–heme, the β band at 528 nm appeared relatively sharp, suggesting partial formation of a six-coordinate heme complex. Upon exposure of the rHSA(HL/L185N)–heme solution to O_2, the UV-vis absorption changed immediately to that of the O_2 adduct complex at 22°C. In contrast, rHSA(HF/L185Q)–heme and rHSA(HF/L185H)–heme were oxidized by O_2, even at low temperature (5°C). After introducing CO gas, all the hemoproteins produced stable carbonyl complexes with identical absorption spectral patterns.

Marked differences are apparent in the comparison of the O_2 binding parameters for rHSA(HL)–heme and rHSA(HL/L185N)–heme. The presence of Asn rather than Leu at position 185 resulted in 18-fold and 10-fold increases in the O_2 binding affinity, respectively, for species I and II (Table 1). These increases were predominantly attributable to the 6–11-fold diminution of the $k_{off}^{O_2}$ values. The high O_2 binding affinity ($P_{1/2}^{O_2}$: 1 Torr) for rHSA(HL/L185N)–heme is now close to that of Hb (R-state) (0.24 Torr) and Mb (0.5 Torr) (Table 1).

Introduction of Leu or Phe into the 186 Position

For rHSA–heme to provide effective O_2 transport *in vivo*, the affinity should be more similar to that of human RBC ($P_{1/2}^{O_2}$: 8 Torr).[23] This requires an O_2 binding affinity that is intermediate between the values of rHSA(HL)–heme and rHSA(HL/L185N)–heme. An effective means to control the O_2 binding affinity of the heme is introduction of a different polar amino acid around the O_2 binding site. A polar Arg-186 exists at the entrance of the heme pocket; we expected that insertion of a nonpolar residue at this position would change the O_2 binding affinity of rHSA–heme. Consequently, we designed new triple mutants, rHSA(HL/R186L) and rHSA(HL/R186F) (Figure 2e,2f).

The MCD in the Soret band region of the ferric rHSA(HL/R186L)–hemin and rHSA(HL/R186F)–hemin both showed low intensity, which is fundamentally equivalent to that observed for rHSA(HL)–hemin. The reduced ferrous form demonstrated the characteristic

UV-vis absorption and MCD spectra of the five-coordinate high-spin complex under an Ar atmosphere. Upon bubbling O_2 gas through the solutions, the spectral patterns were shifted to that of the O_2 adduct complex. The distinct features of all the spectra were quite similar to those of the rHSA(HL)–heme. Fortunately, the O_2 binding affinities of rHSA(HL/R186L)–heme and rHSA(HL/R186F)–heme were more similar to that of human RBC ($P_{1/2}^{O_2}$: 8 Torr) (Table 1). We can conclude that the Arg-186 is an important key amino acid to control the O_2 binding property of the heme and the obtained triple mutants could become RBC substitutes.

Conclusion

We have shown clearly that rHSA–heme can be engineered to bind O_2 reversibly. However, the complex did not display optimal O_2 binding affinity. By emphasizing modification on the distal side of the heme pocket in rHSA, we have prepared distinct rHSA(triple mutant)–heme complexes with a broad range of O_2 binding affinities. The highest affinity mutant rHSA(HL/L185N) contains Asn-185, which has a short amide side-chain that enhances the O_2 binding affinity. On the other hand, introduction of the larger Gln and His side-chains at position 185 partly provided a six-coordinate heme character, and did not stabilize O_2 binding. In a different approach, substitution of Arg-186 at the entrance of the heme pocket with Leu or Phe provided a useful reduction in the O_2 binding affinity, yielding $P_{1/2}^{O_2}$ values that are closely resemble that of the human RBC.

The transport of O_2 by rHSA–heme could be of great clinical importance, not only as a blood substitute, but also as an O_2-providing therapeutic reagent. If the HSA-based O_2 carrier is realized, it has the potential of acting not only as a RBC substitute, but also as an O_2 providing therapeutic reagent.

This work was supported by PRESTO "Control of Structure and Functions", JST, and Health Science Research Grants (Regulatory Science) from MHLW Japan. The work at Imperial College London was partially carried out through the Japan-UK Research Cooperative Program (Joint Project) of JSPS. The authors acknowledge to Dr. Stephen Curry and Dr. Patricia A. Zunszain for their valuable suggestions related to molecular designs of the rHSA mutants and site-directed mutagenesis.

References

[1] Peters Jr., T. *"All about Albumin, Biochemistry, Genetics and Medical Applications"*, Academic Press, San Diego 1997.

[2] (a) U. Kragh-Hansen, *Pharmacol. Rev.* **1981**, *33*, 17. (b) U. Kragh-Hansen, *Danish Med. Bull.* **1990**, *37*, 57.

[3] (a) S. Curry, H. Madelkow, P. Brick, N. Franks, N. *Nat. Struct. Biol.* **1998**, *5*, 827. (b) A. A. Bhattacharya, T. Grune, S. Curry, *J. Mol. Biol.* **2000**, *303*, 721.

[4] J. Ghuman, P. A. Zunszain, I. Petipas, A. A. Bhattacharya, M. Otagiri, S. Curry, *J. Mol. Biol.* **2005**, *353*, 38.

[5] P. A. Adams, M. C. Berman, *Biochem. J.* **1980**, *191*, 95.

[6] M. C. Marden, E. S. Hazard, L. Leclerc, Q. H. Gibson, *Biochemistry* **1989**, *28*, 4422.

[7] T. Komatsu, Y. Matsukawa, E. Tsuchida, *Bioconjugate Chem.* **2002**, *13*, 397.

[8] He, X. M.; Carter, D. C. *Nature* **1992**, *358*, 209–215.

[9] P. A. Zunszain, J. Ghuman, T. Komatsu, E. Tsuchida, S. Curry, *BMC Struct. Biol.* **2003**, *3*: 6.

[10] M. Wardell, Z. Wang, J. X. Ho, J. Robert, F. Ruker, J. Rubel, D. C. Carter, *Biochem. Biophys. Res. Commun.* **2002**, *291*, 813.

[11] (a) T. Komatsu, N. Ohmichi, P. A. Zunszain, S. Curry, E. Tsuchida, *J. Am. Chem. Soc.* **2004**, *126*, 14304. (b) T. Komatsu, N. Ohmichi, A. Nakagawa, P. A. Zunszain, S. Curry, E. Tsuchida, *J. Am. Chem. Soc.* **2005**, *127*,15933.

[12] L. Vickery, T. Nozawa, K. Sauer, *J. Am. Chem. Soc.* **1976**, *98*, 343.

[13] E. Antonini, M. Brunori, M. *"Hemoglobin and Myoglobin in Their Reactions with Ligands"*; North-Holland Pub., Amsterdam 1971; pp 18.

[14] T. G. Traylor, C. K. Chang, J. Geibel, A. Berzinis, T. Mincey, J. Cannon, *J. Am. Chem. Soc.* **1979**, *101*, 6716.

[15] J. P. Collman, J. I. Brauman, B. L. Iverson, J. L. Sessler, R. M. Moris, Q. H. Gibson, *J. Am. Chem. Soc.* **1983**, *105*, 3052.

[16] T. G. Traylor, S. Tsuchiya, D. Campbell, M. Mitchel, D. Stynes, N. Koga, *J. Am. Chem. Soc.* **1985**, *107*, 604.

[17] Q. H. Gibson, *J. Biol. Chem.* **1970**, *245*, 3285.

[18] J. H. Olson, M. E. Andersen, Q. H. Gibson, *J. Biol. Chem.* **1971**, *246*, 5919.

[19] R. Rohlfs, A. J. Mathews, T. E. Carver, J. S. Olson, B. A. Springer, K. D. Egeberg, S. G. Sliger, *J. Biol. Chem.* **1990**, 265, 3168.

[20] S. E. V. Phillips, B. P. Schoenborn, *Nature* **1981**, *292*, 81.

[21] J. S. Olson, A. J. Mathews, R. J. Rohlfs, B. A. Springer, K. D. Egeberg, S. G. Sligar, J. Tame, J.-P. Renaud, K. Nagai, *Nature* **1988**, *336*, 365.

[22] T. Komatsu, A. Nakagawa, P. A. Zunszain, S. Curry, E. Tsuchida, *J. Am. Chem. Soc.* **2007**, *129*, in press.

[23] K. Imai, H. Morimoto, M. Kotani, H. Watari, W. Hirata, M. Kuroda, *Biochim. Biphys. Acta.* **1970**, *200*, 189.

ohio1/ybc-ybc/ybc-ybc/ybc99907/ybc2461d07z | xppws | 23:ver.3 | 1/7/08 | 20:23 | Msc: bc-2007-00400n | TEID: ajk00 | BATID: bc1a60

O_2 Binding to Human Serum Albumin Incorporating Iron Porphyrin with a Covalently Linked Methyl-L-Histidine Isomer

Akito Nakagawa,[†] Teruyuki Komatsu,*[,†,‡] Makoto Iizuka,[†] and Eishun Tsuchida*[,†]

Research Institute for Science and Engineering, Waseda University, 3-4-1 Okubo, Shinjuku-ku, Tokyo 169-8555, Japan, and PRESTO, Japan Science and Technology Agency (JST), 4-1-8 Honcho, Kawaguchi-shi, Saitama 332-0012, Japan. Received October 30, 2007; Revised Manuscript Received December 1, 2007

We describe the significant difference in the O_2 binding affinities of human serum albumin (HSA) incorporating 5,10,15,20-tetrakis{α,α,α,α-*o*-(1′-methylcyclohexanamido)phenyl}porphinatoiron(II) with a covalently linked 1-methyl-L-histidine or 3-methyl-L-histidine [HSA-FeP(1-MHis), HSA-FeP(3-MHis)]. The HSA-FeP(3-MHis) showed an extraordinarily high O_2 binding affinity ($P_{1/2}$ = 0.2 Torr, 25 °C, pH 7.4), which is close to those of relaxed-state hemoglobin and myoglobin. However, replacement of the 3-methyl-L-histidine moiety in FeP(3-MHis) by 1-methyl-L-histidine caused a 35-fold reduction in O_2 affinity; the $P_{1/2}$ value of HSA-FeP(1-MHis) (22 Torr, 37 °C, pH 7.4) is almost identical to that of human red blood cells. Results of kinetic studies indicate that the low O_2 binding affinity of FeP(1-MHis) is predominantly manifested in the high O_2 dissociation rate constant. In a toluene solution, an identical relationship in the O_2 binding property was similarly observed for FeP(1-MHis) and FeP(3-MHis). The axial Fe-N(1-MHis) coordination might be restrained by steric interaction between the 4-methylene group of the histidine and the porphyrin plane.

INTRODUCTION

Numerous synthetic model hemes have been prepared to mimic the O_2 binding capability of hemoglobin (Hb) and myoglobin (Mb) over the past few decades (*1–3*). In these highly modified iron(II) porphyrins, axial coordination of the nitrogenous base plays a crucial role in regulating O_2 binding affinity. Collman and co-workers demonstrated that picket-fence porphyrin[1] ligating a 1,2-dimethylimidazole (1,2-DMIm) showed a 70-fold lower O_2 binding affinity [$P_{1/2}$ (O_2 partial pressure at which 50% of porphyrin was dioxygenated) = 38 Torr, 25 °C] than that of the complex with 1-methylimidazole (1-MIm) (*4, 5*). This reduction was ascribed to the steric interaction between the 2-methyl group of the imidazole and the porphyrin plane. Furthermore, they showed that the replacement of imidazole by pyridine in the tailed picket-fence porphyrin lowered the O_2-binding affinity by a factor of 40 (*6*). The weaker π-basicity of pyridine and the increased steric repulsion of the six-atom pyridine ring compared to that of the five-atom imidazole reduced the O_2 binding of the iron(II) porphyrins (*7–10*). We previously reported that 2-[{8-*N*-(methylimidazolyl)octanoyloxy}methyl]-5,10,15,20-tetrakis{α,α,α,α-*o*-(1′-methylcyclohexanamido)phenyl}porphinatoiron(II) [FeP(2-MIm)] formed a stable O_2 adduct in toluene solution, and human serum albumin (HSA) incorporating FeP(2-MIm) [HSA-FeP(2-MIm)] can bind O_2 not only in aqueous media (pH 7.4) but also in the blood stream as an artificial red blood cell (RBC) substitute (*11, 12*). For practical biomedical applications of the synthetic iron(II) porphyrin as an O_2 carrier, two physiological requirements exist. First, O_2 binding affinity should be close to that of human RBC ($P_{1/2}$ = 27 Torr, 37 °C). Second, it is favorable to use natural histidine as an axial base because some imidazole and pyridine derivatives show toxicity to respiratory organs and the central nervous system (*13*). Nevertheless, few studies have addressed O_2 binding of the synthetic model heme having a histidyl group (*14–16*). We have demonstrated the O_2 binding equilibrium and kinetics of 5,10,15,20-tetrakis{α,α,α,α-*o*-(1′-methylcyclohexanamido)phenyl}porphinatoiron(II) with an ω-histidylalkyl chain [FeP(His)[2]] (*17*). A new class of biocompatible O_2 carriers would be realized if we can regulate O_2 binding affinity by changing the steric and electronic natures of the attached histidine. We now report a significant difference in the O_2 binding properties of HSA hybrid with synthetic iron(II) porphyrin bearing a covalently linked 1-methyl-L-histidine or 3-methyl-L-histidine [HSA-FeP(1-MHis) and HSA-FeP(3-MHis)] (Figure 1) under physiological conditions (pH 7.4, 37 °C).

The 1-methyl-L-histidine methylester or 3-methyl-L-histidine methylester was introduced into the carboxyl group of the parent free-base porphyrin, 2-{(4-carboxybutanoyloxy)methyl}-5,10,15,20-tetrakis{α,α,α,α-*o*-(1′-methylcyclohexanamido)phenyl}porphin [2HP(COOH)] (*11*), via an amide linkage, yielding histidine-terminated porphyrins (>60% yield) (Figure 1). The cyclohexanoyl substituents stabilized the O_2 adduct complex rather than the pivaloy group (*11*). The central iron was inserted as iron(II) using $FeBr_2$ and 2,6-lutidine in anhydrous THF. The analytical data of all compounds were satisfactorily obtained (see Supporting Information).

Both FeP(1-MHis) and FeP(3-MHis) are readily incorporated into HSA (Mw: 66.5 kDa), producing stable artificial hemoproteins: HSA-FeP(1-MHis) and HSA-FeP(3-MHis) [in phos-

* Corresponding author. Tel: +81-3-5286-3120. Fax: +81-3-3205-4740. E-mail: eishun@waseda.jp (E.T.). E-mail: teruyuki@waseda.jp (T.K.).

[†] Waseda University.

[‡] Japan Science and Technology Agency (JST).

[1] Picket-fence porphyrin: 5,10,15,20-tetrakis{(α,α,α,α-o-pivalamido)-phenyl}porphinatoiron.

[2] Abbreviations: FeP(His), 2-{(4-methoxycarbonyl-histidinamidobutanoyloxy)methyl}-5,10,15,20-tetrakis{α,α,α,α-o-(1′-methyl)cyclohexanamido)phenyl}porphinatoiron; FeP(1-MHis),2-[{4-methoxycarbonyl(1-methyl)histidinamidobutanoyloxy}methyl]-5,10,15,20-tetrakis{α,α,α,α-o-(1′-methyl)cyclohexanamido)phenyl}porphinatoiron; FeP(3-MHis),2-[{4-methoxycarbonyl(3-methyl)histidinamidobutanoyloxy}methyl]-5,-10,15,20-tetrakis{α,α,α,α-o-(1′-methylcyclohexanamido)phenyl}porphinatoiron.

10.1021/bc700400n CCC: $37.00

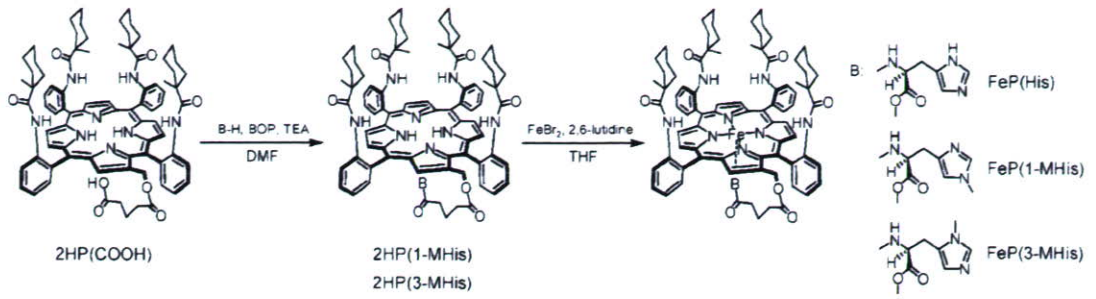

Figure 1. Synthetic scheme of iron(II) porphyrin bearing a covalently linked histidine derivative as an axial base at the β-pyrrolic position.

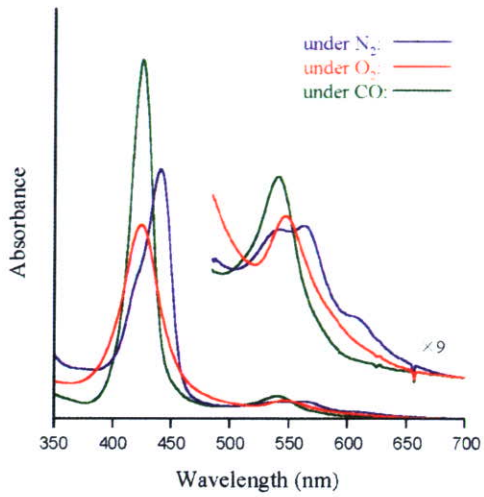

Figure 2. UV–vis absorption spectral changes of HSA-FeP(1-MHis) in PBS solution at 25 °C.

phate-buffered saline (PBS) solution at pH 7.4, [porphyrin]/[HSA] = 4 (mol/mol)]. The UV–vis absorption spectra of the aqueous HSA-FeP(1-MHis) and HSA-FeP(3-MHis) solutions under an N_2 atmosphere showed a similar feature of HSA-FeP(2-MIm) and HSA-FeP(His) (Figure 2) (Table S1) (*11, 17*). The spectral shapes resembled those of the five-N-coordinate high-spin ferrous complex of picket-fence porphyrin and other tetraphenylporphyrin derivatives (*5*). These results indicated that FeP(1-MHis) and FeP(3-MHis) formed a five-N-coordinate high-spin complex with an intramolecularly coordinated methyl-L-histidine moiety in the protein matrix. Upon bubbling of O_2 gas into the solution, the absorption pattern changed immediately to that of the O_2 adduct complex. The dioxygenations of these artificial hemoproteins have been observed reversibly under physiological conditions (pH 7.4, 37 °C). After passing the CO gas, the absorption maxima shifted to that of the carbonyl complex.

The O_2 binding affinities [$K = (P_{1/2})^{-1}$] of HSA-FeP(1-MHis) and HSA-FeP(3-MHis) were determined by the absorption spectral changes at various O_2 concentrations (eq 1).

$$\mathrm{FeP(B)} + \mathrm{O_2} \underset{k_{off}}{\overset{k_{on}}{\rightleftharpoons}} \mathrm{FeP(B)\text{-}O_2} \qquad [K = (P_{1/2})^{-1}] \tag{1}$$

The HSA-FeP(3-MHis) showed an extraordinarily high O_2 binding affinity ($P_{1/2}$ = 0.2 Torr, 25 °C), which is 5-fold greater than that of HSA-FeP(His), which was close to the values of the relaxed-state Hb(α) and Mb (Table 1) (*18–20*). However, replacement of the 3-methyl-L-histidine moiety in FeP(3-MHis) by the 1-methyl-L-histidine isomer [FeP(1-MHis)] caused a 35-fold reduction of O_2 binding affinity ($P_{1/2}$ = 7 Torr, 25 °C); the

Table 1. O_2 Binding Parameters of Human Serum Albumin Hybrid with Iron(II) Porphyrin Bearing a Methyl-L-Histidine Isomer in PBS Solution (pH 7.4) at 25 °C

HSA-iron(II) porphyrin	k_{on} (M^{-1} s^{-1})	k'_{on} (M^{-1} s^{-1})	k_{off} (s^{-1})	k'_{off} (s^{-1})	$P_{1/2}$[a] (Torr)
HSA-FeP(1-MHis)	5.4×10^7	8.1×10^6	620	93	7 (22)
HSA-FeP(3-MHis)	5.4×10^7	6.8×10^6	20	2.4	0.2 (1)
HSA-FeP(His)[b]	5.4×10^7	8.8×10^6	89	14	1 (3)
Hb(α) (R-state)[c]	3.3×10^7[d]		13[e]		0.24
Mb[f,g]	1.4×10^7		12		0.51
RBC[h]					8 (27)

[a] At 37 °C in parenthesis. [b] Ref *11*. [c] Human Hb α-subunit. [d] In 0.1 M phosphate buffer (pH 7.0, 21.5 °C); ref *18*. [e] In 10 mM phosphate buffer (pH 7.0, 20 °C); ref *19*. [f] Sperm whale Mb. [g] In 0.1 M phosphate buffer (pH 7.0, 20 °C); ref *20*. [h] Human red blood cell suspension. In isotonic buffer (pH 7.4); ref *21*.

$P_{1/2}$ value of 22 Torr at 37 °C was almost identical to that of human RBC (27 Torr) (*21*).

Laser flash photolysis experiments gave the association and dissociation rate constants for O_2 (k_{on}, k_{off}) (*5, 11*). The time course of the absorption change accompanying the O_2 recombinations to HSA-FeP(1-MHis) and HSA-FeP(3-MHis) after the laser pulse irradiation comprised two phases of first-order kinetics (Figure S1a). The decay was fitted by a double exponential profile, which provided the fast and slow association rate constants of O_2 (k_{on} and k'_{on}) (Table 1). This behavior was similarly observed in HSA-FeP(His) and HSA-FeP(2-MIm) (*11*). It has been interpreted that the O_2 associations to the iron(II) porphyrins in HSA were affected by microenvironments around the accommodation site (steric hindrance of the amino acid residue and difference in polarity) (*22*). The kinetic data indicated that the low O_2 binding affinity of HSA-FeP(1-MHis) is predominantly manifested in the high O_2 dissociation rate constant (Table 1).

To evaluate the significant differences in FeP(1-MHis) and FeP(3-MHis), their O_2 binding parameters in toluene solution were determined. The UV–vis absorption spectra of ferrous FeP(1-MHis) (λ_{max}, 440, 542, 563 nm) and FeP(3-MHis) (λ_{max}, 440, 540, 565 nm) under an N_2 atmosphere showed the formation of a five-N-coordinate high spin complex. Dioxygenation was sufficiently stable and reversible at 25 °C depending on O_2 partial pressure. The recombination process of O_2 to the iron(II) porphyrins in toluene solution after laser flash photolysis was fitted by a single exponential (Figure S1b). FeP(3-MHis) exhibited a 6-fold higher O_2 binding affinity ($P_{1/2}$ = 0.3 Torr, 25 °C) compared to that of FeP(His) (Table 2) (*11*). Kinetically, this high O_2 binding affinity is attributable to the low O_2 dissociation rate. The high σ-basicity of 3-methyl-L-histidine (p*K*a, 6.48) in comparison to that of histidine (p*K*a, 6.00) (*23*) can serve to increase the electron density on the central metal, which would enhance O_2 uptake. FeP(1-MHis) showed a 90-fold lower O_2 affinity ($P_{1/2}$ = 27 Torr, 25 °C) relative to FeP(3-MHis), which is mainly caused by the high k_{off} value, as observed in aqueous media. In general, the steric

Table 2. O_2 Binding Parameters of Iron(II) Porphyrin Bearing a Methyl-L-Histidine in Toluene Solution at 25 °C

iron(II) porphyrin	k_{on} (M^{-1} s^{-1})	k_{off} (s^{-1})	$P_{1/2}$ (Torr)
FeP(1-MHis)	9.8×10^7	3.5×10^4	27
FeP(3-MHis)	1.6×10^8	5.2×10^2	0.3
FeP(His)[a]	2.0×10^8	4.3×10^3	1.7

[a] In benzene solution, ref *17*.

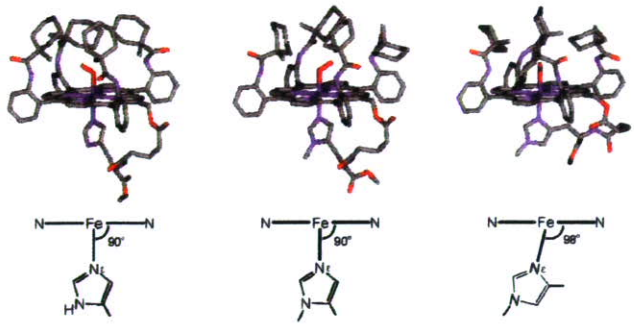

Figure 3. Simulated structures of the O_2 adduct complexes of FeP(His), FeP(3-MHis), and FeP(1-MHis). In FeP(His) and FeP(3-MHis), the bond angles of N(por)−Fe−N(His) were 90°, but 98° in FeP(1-MHis) because of the steric interaction between the 4-methylene group of histidine and the porphyrin plane. Molecular dynamics and minimization (force field: esff) were performed using an Insight II system. Hydrogens were omitted for clarification.

hindrance to the axial base coordination deforms the six-coordinate structure of the iron(II) porphyrin and increases the O_2 dissociation rate constant (*1, 2*). For example, the 1,2-DMIm complexes showed 11–58-fold higher k_{off} values than the 1-MIm ligated complexes (*3, 5, 24*).

We simulated the geometry of histidine coordination in dioxygenated porphyrin.[3] The bond angle of N(por)−Fe−N(His) was 90° for FeP(His) and FeP(3-MHis), but it was markedly tilted in FeP(1-MHis) (a maximum of 98°) (Figure 3). On the basis of these results, it can be concluded that the axial coordination of 1-methyl-L-histidine to the central iron is restrained by the steric interaction between the 4-methylene group of the histidine and the porphyrin plane, which significantly increased the dissociation rate of O_2.

In conclusion, a variation in the methyl-L-histidine isomer covalently linked at the porphyrin periphery changed the O_2 binding affinity of the iron(II) porphyrin by a factor of 90 in toluene. This difference is greater than the previous finding for a picket-fence porphyrin (2-MIm) complex-bound O_2 with a 70-fold lower affinity than that of the 1-MIm complex (*4*). The increased k_{off} value of FeP(1-MHis) is caused by steric repulsion between the 4-methylene group of histidine and the porphyrin plane. In aqueous media, the O_2 binding ability of HSA incorporating the iron(II) porphyrin can also be modulated by structural isomerization of the axial methyl-L-histidine. HSA-FeP(1-MHis) with a $P_{1/2}$ value similar to that of human RBC under physiological conditions can become a promising O_2 carrier, which satisfies both the biocompatibility and clinical requirements for efficient O_2 delivery to the tissue cells.

ACKNOWLEDGMENT

This work was partially supported by Grant-in-Aid for Young Scientists (B) (No. 18750156) from JSPS, PRESTO from JST, and Health Science Research Grants from MHLW, Japan.

[3] The esff forcefield simulation was performed using an Insight II system (Molecular Simulations Inc.). The structure was generated by alternative minimizations and annealing dynamic calculations from 1,000 to 100 K.

Supporting Information Available: Experimental details, absorption maximum wavelengths of the iron(II) porphyrins, and absorption change accompanying O_2 rebinding to FeP(3-MHis) and HSA-FeP(3-MHis) after laser flash photolysis. This material is available free of charge via the Internet at http://pubs.acs.org.

LITERATURE CITED

(1) Collman, J. P., Boulatov, R., Sunderland, C. J., and Fu, L. (2004) Functional analogues of cytochrome c oxidase, myoglobin, and hemoglobin. *Chem. Rev. 104*, 561–588.
(2) Collman, J. P., and Fu, L. (1999) Synthetic Models for Hemoglobin and Myoglobin. *Acc. Chem. Res. 32*, 455–463.
(3) Momenteau, M., and Reed, C. A. (1994) Synthetic heme-dioxygen complexes. *Chem. Rev. 94*, 659–698.
(4) Collman, J. P., Brauman, J. I., Doxsee, K. M., Halberd, T. M., and Suslick, K. S. (1978) Model compounds for the T state of hemoglobin. *Proc. Natl. Acad. Sci. U.S.A. 75*, 564–568.
(5) Collman, J. P., Brauman, J. I., Iverson, B. L., Sessler, J. L., Morris, R. M., and Gibson, Q. H. (1983) O_2 and CO binding to iron(II) porphyrins: A comparison of the "picket fence" and "pocket" porphyrins. *J. Am. Chem. Soc. 105*, 3052–3064.
(6) Collman, J. P., Brauman, J. I., Doxsee, K. M., Sessler, J., Morris, R. M., and Gibson, Q. H. (1983) Effect of axial base on dioxygen and carbon monoxide affinities of iron(II) porphyrins. Imidazole vs. pyridine. *Inorg. Chem. 22*, 1427–1432.
(7) Chang, C. K., and Traylor, T. G. (1975) Kinetics of oxygen and carbon monoxide binding to synthetic analogs of the myoglobin and hemoglobin active sites. *Proc. Nat. Acad. Sci. U.S.A. 72*, 1166–1170.
(8) Linard, J. E., Ellis, P. E., Jr., Budge, J. R., Jones, R. D., and Basolo, F. (1980) Oxygenation of iron(II) and cobalt(II) "capped" porphyrins. *J. Am. Chem. Soc. 102*, 1896–1904.
(9) Momenteau, M., Mispelter, J., Loock, B., and Lhoste, J.-M. (1985) Both-faces hindered porphyrins. Part 3. Synthesis and characterization of internally five-co-ordinated iron(II) basket handle porphyrins derived from 5,10,15,20-tetrakis(o-aminophenyl)porphyrin. *J. Chem. Soc., Perkin Trans.1* 221–231.
(10) Lavalette, D., Tetreau, C., Mispelter, J., Momenteau, M., and Lhoste, J.-M. (1984) Linear free-energy relationships in binding of oxygen and carbon monoxide with heme model compounds and heme proteins. *Eur. J. Biochem. 145*, 555–565.
(11) Komatsu, T., Matsukawa, Y., and Tsuchida, E. (2002) Effect of heme structure on O_2-binding properties of human serum albumin-heme hybrids: Intramolecular histidine coordination provides a stable O_2-adduct complex. *Bioconjugate Chem. 13*, 397–402.
(12) Komatsu, T., Huang, Y., Yamamoto, H., Horinouchi, H., Kobayashi, K., and Tsuchida, E. (2004) Exchange transfusion with synthetic oxygen-carrying plasma protein "albumin-heme" into an acute anemia rat model after seventy-percent hemodilution. *J. Biomed. Mater. Res. 71A*, 644–651.
(13) Sax, N. I., and Lewis, R. J. (1987) *Hazardous Chemicals Desk Reference*, Van Nostrand Reinhold Company, Inc., New York.
(14) Van der Heijden, A., Peter, H. G., and Van der Oord, A. H. A. (1971) Coupling of L-histidine methyl ester and L-histidine-containing peptide esters to ferric protoporphyrin IX chloride. *J. Chem. Soc. D* 369–370.
(15) Warme, P. K., and Hager, L. P. (1970) Heme sulfuric anhydrides. I. Synthesis and reactions of mesoheme sulfuric anhydride. *Biochemistry 9*, 1599–1606.
(16) Momenteau, M., Rougee, M., and Loock, B. (1976) Five-coordinate iron-porphyrin as a model for the active site of hemoproteins. Characterization and coordinating properties. *Eur. J. Biochem. 71*, 63–76.
(17) Komatsu, T., Matsukawa, Y., Miyatake, K., and Tsuchida, E. (2001) O_2-adduct complex of meso-tetrakis(α,α,α,α-o-pivalamidophenyl)porphinatoiron(II) with an intramolecularly coordinated proximal histidine. *Chem. Lett.* 668–669.
(18) Gibson, Q. H. (1970) The reaction of oxygen with hemoglobin and the kinetic basis of the effect of salt on binding of oxygen. *J. Biol. Chem. 245*, 3285–3288.

(19) Olson, J. S., Andersen, M. E., and Gibson, Q. H. (1971) The Dissociation of the first oxygen molecule from some mammalian oxyhemoglobins. *J. Biol. Chem. 246*, 5919–5923.

(20) Rohlfs, R., Mathews, A. J., Carver, T. E., Olson, J. S., Springer, B. A., Egeberg, K. D., and Sligar, S. G. (1990) The effects of amino acid substitution at position E7 (residue 64) on the kinetics of ligand binding to sperm whale myoglobin. *J. Biol. Chem. 265*, 3168–3176.

(21) Imai, K., Morimoto, H., Kotani, M., Watari, H., Hirata, W., and Kuroda, M. (1979) Studies on the function of abnormal hemoglobins I. An improved method for automatic measurement of the oxygen equilibrium curve of hemoglobin. *Biochim., Biophys. Acta 200*, 189–1967.

(22) Komatsu, T., Matsukawa, Y., and Tsuchida, E. (2000) Kinetics of CO and O_2 binding to human serum albumin-heme hybrid. *Bioconjugate Chem. 11*, 772–776.

(23) Lide, R. D., Eds. (2000) *CRC Handbook of Chemistry and Physics*, 81st ed., Section 7, CRC Press, Boca Raton, FL.

(24) Momenteau, M., Loock, B., Tetreau, C., Lavalette, D., Croisy, A., Schaeffer, C., Huel, and Lhoste, J.-M. (1987) Synthesis and characterization of a new series of iron(II) single-face hindered porphyrins. Influence of central steric hindrance upon carbon monoxide and oxygen binding. *J. Chem. Soc., Perkin Trans. 2* 249–257.

BC700400N

Review

Hemoglobin Vesicles to Treat Critical Ischemia

Dominique Erni, Reto Wettstein, Claudio Contaldo, Jan A. Plock, Nassim Rafatmehr, Hiromi Sakai* and Eishun Tsuchida*

Abstract

The initital purpose for developing artificial oxygen carriers was to replace blood transfusions in order to avoid their adverse effects such as immunologic reactions, transmission of infectious diseases, limited availability and restricted storage conditions. With the advent of new generations of artifical oxygen carriers, a shift of paradigm evolved that considers the artificial oxygen carriers as oxygen therapeutics re-distributing oxygen delivery in the favor of tissues in need. This function may find a particular application in tissues rendered hypoxic due to arterial occlusive diseases. This review, based on a large series of intravital microscopy studies in a hamster skin flap model, outlines the optimal design of hemoglobin vesicles (HbVs) given for the above intention. In summary, the HbV should be of a large diameter, and oxygen affinity, colloid osmotic pressure and viscosity of the HbV solution should be high.

Keywords artificial oxygen carrier, intravital microscopy, skin flap, hypoxia, hemodilution

Introduction

The initital drive to develop artificial oxygen carriers was to reduce the need of blood transfusions in order to circumvent their drawbacks such as immunologic reactions, blood-borne transmitted diseases, limited availability and restricted storage time[1-3]. The first generation artificial blood substitutes included modified hemoglobin (Hb) molecules and perfluorocarbons. The Hb-based oxygen carriers (HBOCs) were designed to mimick the physiological function of red blood cells in terms of oxygen uptake, transport and release. Accordingly, their physicochemical properties were targeted to that of human blood.

However, on a clinical level, the artificial blood substitutes have failed to meet the expectations so far. Clinical trials yielded serious adverse effects, which were mainly related to an unwanted vasoconstrictor response to the Hb molecules[1-4]. There was an urge to invent new HBOCs, which was achieved by introducing a variety of structural modifications of the hemoglobins and the rheological properties of the solvent[1,2,5]. This evolution was paralleled by a shift of paradigm regarding the function of artificial oxygen carriers: they were no longer seen as mere oxygen transporters and suppliers but rather as oxygen therapeutics in a sense that they would influence the distribution of RBC-bound oxygen in favor of the tissues in need[2,5].

This new paradigm went along with the idea of using artificial oxygen-carrying solutions as drugs instead of blood substitutes, thus revealing new therapeutic strategies. One of them consists in the treatment of local tissue hypoxia caused by arterial occlusion. Although occlusive vascular diseases account for the highest causes of death and some of the highest rates of morbidity and health care costs in the industrialized countries, little emphasis has been put on translational research focused on this indication for artificial oxygen carriers. Symptomatically, this is not either the issue in any of the ongoing clinical trials[3]. Some experimental experience with this therapeutic strategy exists mostly for first generation HBOCs and perfluorocarbons, both of which yielded beneficial effects in acute ischemic hypoxia in cerebral[6-11], myocardial[12-15] and peripheral[16] tissues. On the other hand, a clinical study testing the effect of diaspirin cross-linked Hb on acute ischemic stroke revealed that treatment with this first generation HBOC was an independent predictor of a worse outcome[4].

In collaboration with Waseda University, we have investigated the efficacy of hemoglobin vesicles (HbVs), a second generation HBOC, in critically ischemic skin flaps. Our goal was to ameliorate hypoxia by improving oxygen delivery with the infusion of HbV solutions. This treatment is supposed to serve as an ancillary measure until adequate

Department of Plastic Surgery, Inselspital, University of Berne, CH-3010 Berne, Switzerland
*Advanced Research Institute for Science and Engineering, Waseda University, Tokyo 169-8555, Japan
論文受付 2007年3月24日　論文受理 2007年4月9日

perfusion is re-established surgically or spontaneously by neo-vascularization. We favored the use of an HBOC because unlike perfluorocarbons, HBOCs do not require high pressure oxygen ventilation, which may be toxic if applied over the prolonged period of time that may be necessary to bridge the ischemic condition[17]. This article reviews our experimental experience with HbVs used for this purpose. Our studies were focused on investigating the effects of the various physicochemical properties of the HbV solutions in order to optimize their design.

Standardized model and HBOC preparation allow for comparable and reproducible findings

In our experiments we used a hamster skin flap model that was derived from the well-established dorsal skinfold chamber, a model that allows for monitoring the hemodynamics and tissue oxygenation on a microscopic level (Fig. 1.)[18,19]. The model simulates critical ischemia in peripheral tissue after acute vascular obstruction of the anatomical, axial blood supply, which renders this tissue dependent on a collateral vascularization. In our model, the

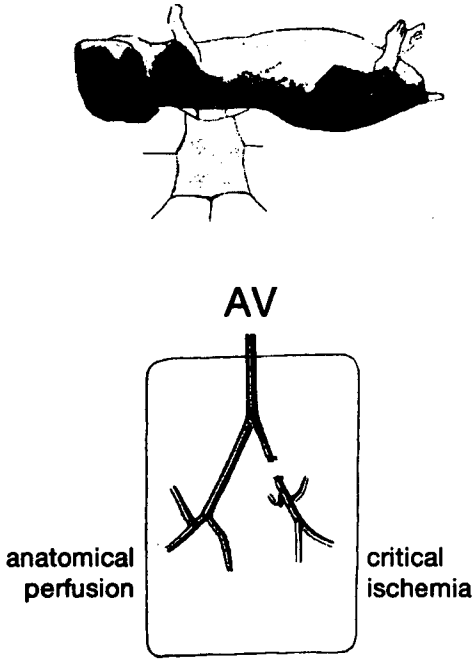

Fig. 1. Schematic view of animal model (*above*). A flap is dissected from the epilated back skin of anesthetized hamsters and mounted on a platform for intravital microscopy. Schematic view of preparation (*below*). The flap is nourished by one artery and vein, which bifurcate into two branches. After transecting the right branch, the corresponding tissue is perfused via collateral vessels connecting the two vascular beds and becomes critically ischemic. Redrawn from Erni et al[18]

critically ischemic tissue showed hypoxia[20], hypoxia-related inflammation[21] and incresaed rates of cell death[22].

The HbVs were produced and provided by Waseda University[23]. They consisted of isolated, purified human Hb originating from outdated RBC concentrates. The Hbs were encapsulated with a double-layer phospholipid membrane that was coated with polethylene-glycol in order to avoid agglutination. The diameter of the HbVs was approximately 250 nm. The oxygen affinity (P50) was regulated by adding the co-encapsulated allosteric effector pyridoxal 5'-phosphate.

To improve microcirculation: a prerequisite

Because the reason for hypoxia in critical ischemia related to arterial occlusive diseases is hypoperfusion, the effect of the oxygen-carrying solution on the microcirculation is of utmost importance. Any further reduction in microcirculatory blood flow may be deleterious. Partly severe vasoconstriction was observed after application of first generation HBOCs[1,2,24,25], which was mainly due to the NO-scavenging effect of plasma-bound Hb[15] but also due to NO-independent mechanisms[26]. The vasoconstrictor effect of the Hb compounds were largely dependent on their size[24]; its increase was therefore one of the first goals to be accomplished with the second generation HBOCs[2]. No vasoconstriction, neither in normally perfused nor in ischemic tissues, and no arterial hypertension were observed in any of the animals receiving HbVs[20,24,25,27-30] which are considered the largest HBOCs.

More than trying to avoid vasoconstriction, the primary goal should be to increase microcirculatory blood flow in the ischemic tissue, since blood flow determines oxygen delivery. In this context, homogenous distribution of blood flow, best expressed by functional capillary density (FCD), is crucial to avoid hypoxic tissue areas in spite of adequate total volumetric flow[31,32]. It has been postulated that the ischemic tissue may benefit from the small size of the artificial oxygen carrier that is still able to penetrate the vasculature through stenoses that are no longer accessible by red blood cells. Although this phenomenon is intellectually appealing and has been described *in vivo*[33], the scientific proof of its biological efficacy is lacking. On the contrary, HbVs were completely inefficient if they were given in a solution that failed to improve microcirculatory blood flow in the ischemic tissue (Fig. 2.)[20], thus emphasizing the importance of the rheological formula of the oxygen-carrying solution. Similar observations have been made in other conditions of compromized microcirculation, where re-establishing microcirculatory blood flow and FCD rather than increasing oxygen-carrying capacity were important in preventing hypoxia[32,34].

In this context, high colloidal osmotic pressure (COP) and

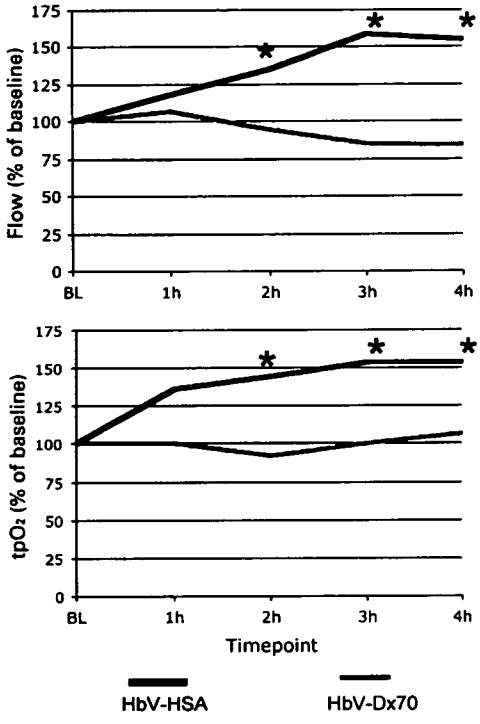

Fig. 2. Mean arteriolar blood flow and partial oxygen tension in the critically ischemic tissue before and after 50% isovolemic blood exchange with HbV dissolved in 8% human serum albumin (HbV-HSA) or 6% dextran 70 (HbV-Dx70). *p < 0.05 vs. Baseline and HbV-HSA. HbVs are not able to improve tissue oxygenation if blood flow is not increased. Redrawnfrom Erni et al[20].

high viscosity proved to be beneficial to both volumetric blood flow and FCD[2,5,20-22,25,32,34,35]. High COP leads to blood volume expansion and subsequent increase in preload, cardiac output and mean arterial blood pressure. Furthermore, hyperoncotic solutions may attenuate fluid extravasation and edema formation in the ischemic tissue, thus relieving edema-related impairment of oxygen diffusion[36-38].

The effects of the viscosity of the HBOC solution appear to be manifold. Whereas we and others have repeatedly demonstrated that the reduction in total blood viscosity during hemodilution is beneficial particularly in conditions of compromized microcirculation[10,20,22,25,30,39,40], it seems to be advantageous to enhance viscosity in the plasma phase[5,21,22,25,41,42]. To prevent from decreasing plasma viscosity below a certain level is crucial in maintaining capillary perfusion pressure, which is explained by the influence of plasma viscosity on NO-mediated, shear stress-induced arteriolar vasodilation[41,43-45]. However, raising plasma viscosity to supraphysiological levels did not reveal any arteriolar vasodilation in our model, whereas microcirculatory blood flow and capillary perfusion were improved[20-22,25,30]. Since this was accompanied by a decrease in capillary diameter, the viscosity-related microcirculatory improvement may have been achieved by a decrease in capillary intraluminal pressure due to a reduction in post-capillary resistance, which in turn is predominantly influenced by the leukocyte-endothelium interaction[46]. It has been reported that leukocyte adhesion, which is the first step in this cascade of events, may be attenuated by increasing shear stress on the endothelium[47], a scenario that is most conceivable considering the increased plasma viscosity after HbV infusion[21,22]. The assumption that HbV solutions improve capillary perfusion by reducing post-capillary leukocyte adhesion and activation was further evidenced by a decrease in inflammatory markers such as endothelial leakage, tumor necrosis factor (TNF)-alpha, interleukin (IL)-6 and tissue leukocyte counts[21,22].

The influence of the oxygen-carrying solution on such inflammatory pathways may not be under-estimated, in particular in view of the ischemia-reperfusion effect that takes place after improving the oxygenation of this tissue. Due to the reduced arterial perfusion pressure, the influence of post-capillary resistance on capillary flow is more relevant if the tissues are indirectly perfused via the collateralized vasculature. Various authors have reported that artificial oxygen carriers may have the potential to attenuate ischemia-reperfusion injury[48,49], in particular if they are supplemented with antioxidants[50].

The principle of improving oxygen delivery by augmenting microcirculatory blood flow is based on the maintenance of adequate tissue perfusion either by the remaining blood flow an incompletely occluded arterial axis or by functional collateral vessels. Collateral vascularization varies between species, individuals, organs and even within organs[51-53]. Most of the existing experimental studies that report a beneficial effect of artificial oxygen carriers on critical ischemia due to arterial occlusion, including those cited in this review, relied on the presence of a functional collateral vasculature. Its importance was highlighted by Rebel et al who found that hemodilution with an oxygen-carrying solution after cerebral artery occlusion was able to increase oxygen delivery in the collateralized cortex but not in the caudate nucleus, which is an end artery territory[9]. The growth of the collateral vasculature, a process termed arteriogenesis, is triggered by a chronic impairment of axial, anatomical blood supply[52]. The collateral vascularization acts as a lifebelt when it comes to a complete shut down of the anatomical perfusion, and the development of therapies that aim at enhancing collateral vascularization has gained great scientific interest in the recent years[54]. It is not unlikely that artficial oxygen carriers

will be playing a pivotal role in the therapeutic concept of oxygenating critically ischemic tissue via a collateralized vasculature in the near future.

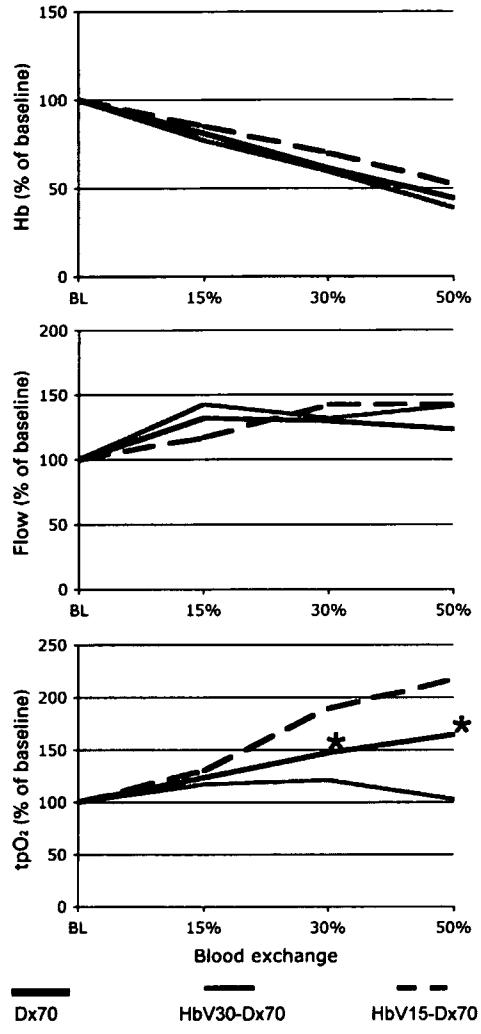

Fig. 3. Mean arterial Hb concentration, and mean arteriolar blood flow and partial oxygen tension in the critically ischemic tissue before and after stepwise isovolemic hemodilution with 6% dextran 70 (Dx70) and HbV dissolved in Dx70. The P50 of HbVs was 30 mmHg (HbV30-Dx70) or 15 mmHg (HbV15-HbV). *$p < 0.05$ vs. other groups. In spite of decreasing Hb concentrations, tissue oxygen tension increases with every step of hemodilution with HbV solutions but not with Dx70. Tissue oxygenation is better for HbV with higher oxygen affinity. Redrawn from Contaldo et al[30].

To make the HBOC increase oxygen delivery to the tissue in need

If the vesicles did not contain Hb, oxygenation and tissue survival in the critically ischemic tissue could not be improved although rheological properties and microcirculatory improvements were similar to the oxygen-carrying vesicle (HbV) solutions[22]. The oxygenation in the critically ischemic tissue was correlated with the HbV concentration in the circulating blood but not with the total Hb concentration (RBC-bound Hb plus HbV-bound Hb)[30]. Furthermore, the contribution of HbV-bound oxygen to the total oxygen extracted by the ischemic tissue was estimated to be less than 10% even at high HbV concentrations[22]. These data suggest that the HbV solution acts rather by promoting the release of RBC-bound oxygen to the ischemic tissue in terms of an oxygen therapeutic than by enhancing the oxygen-carrying capacity in terms of a RBC substitute. The HbVs circulate in the plasma phase, thus interfering with the oxygen delivery from the RBCs to the tissue[55,56]. According to the Stokes-Einstein equation, the diffusivity of oxygen is inversely proportional to the size of the plasma-bound oxygen-carrying compound and the viscosity of the plasma suspension. Furthermore, oxygen diffusivity is negatively affected by the oxygen affinity of the oxygen carrier, and high oxygen affinity shifts oxygen release towards the downstream direction[28,31,57]. In our studies, we have repeatedly demonstrated that increasing the size and oxygen affinity of the oxygen carrier as well as the plasma viscosity exerts a positive effect on the oxygenation in the critically ischemic tissue[21,22,25,30]. This strongly suggests that the benefit was obtained by the maintaining oxygen content high in the blood entering the critically ischemic tissue, which is achieved by impeding unnecessary oxygen loss to the normoxic tissue in the upstream vasculature, whereas the increased oxygen retention is over-ruled by the high oxygen tension gradient between blood and tissue being present in a hypoxic environment. The result is a net re-distribution of oxygen in favor of the critically ischemic tissue, which is the more efficient the more oxygen is kept intraluminaly upstream. In our model, the upstream oxygen loss was estimated at 40-50%[19,28]. It may be even higher in species with higher arterial oxygen saturation (SaO_2 is approximately 80% in our model), or in tissues with a higher rate of oxygen extraction.

Equipped with the above-mentioned physicochemical requirements, the HbVs were able to improve microcirculation, oxygenation and tissue survival, and to attenuate hypoxia-related inflammation in the critically ischemic tissue without necessitating the microcirculatory benefit obtained by hemodilution and volume expansion (Fig. 4.)[21]. This was accomplished in terms of a topload infusion, which is a more appropriate mode of application in the clinical setting because blood exchange and adverse effects related to hypervolemia can be avoided.

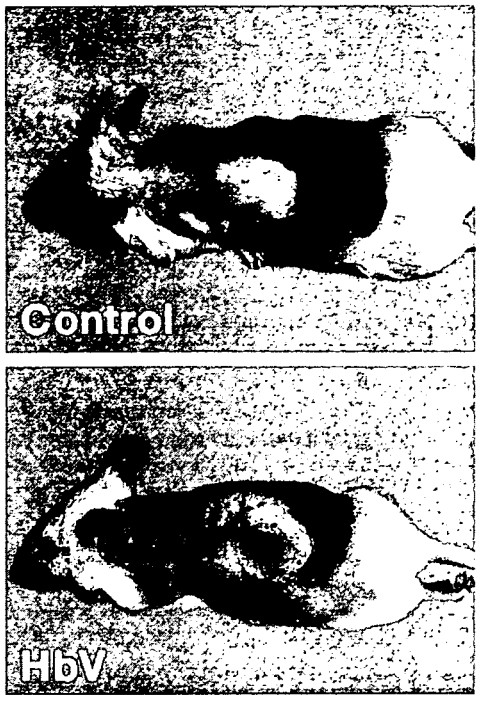

Fig. 4. Cranially based bilateral skin flaps were raised on the dorsum of mice. In the untreated control animals, about the distal two thirds of the flap surface necrotized due to critical ischemia (*above*). Flap survival was markedly improved after topload infusion of HbV dissolved in saline (Hb concentration 10g/dl, 25% total blood volume (*below*).

Summary

Based on a large set of experimental data, the optimal profile of an HBOC solution determined to improve oxygenation, functionality and integrity of critically ischemic tissue can be outlined as follows:

1) The hemoglobin compound should be of a large diameter in order to prevent vasoconstriction due to extravasation.
2) The viscosity of the solution should be high in order to promote shear stress-related vasodilation and to diminish leukocyte- endothelium interactivity.
3) The oxygen affinity of the HBOC should be high in order to improve oxygen distribution, which is also positively influenced by increasing the size of the Hb compounds and the viscosity of the Hb solutions.

Furthermore, the efficacy of HBOC solutions are greatly dependent on a functional collateral vascularization of the ischemic tissue.

Acknowledgements

This research was supported by the Swiss National Foundation for Scientific Research (Grants No. 32-054092.98 and 32-065149.01, 32-050771.97, 32-10840805), the Department of Clinical Research, University of Berne, Switzerland, and by Health Sciences Research (Research on Regulatory Science, H18-IYAKU-Ippan-021, 022) from the Ministry of Health, Labour and Welfare, Japan, Grants in Aid for Scientific Research from the Japan Society for the Promotion of Science and Oxygenix Inc. H.S. and E.T. are consultants of Oxygenix Inc.

References

1. Chang TM. Artificial cells for cell and organ replacements. Artif Organs 2004;28:265-70.
2. Winslow RM. Current status of blood substitute research: towards a new paradigm. J Intern Med 2003;253:508-17.
3. Winslow RM. Current status of oxygen carriers ("blood substitutes"): 2006. Vox Sanguinis 2006;91:102-10.
4. Saxena R, Wijnhoud AD, Carton H, Hacke W, Kaste M, Przybelski RJ, Stern KN, Koudstaal PJ. Controlled safety study of a hemoglobin-based oxygen carrier, DCLHb, in acute ischemic stroke. Stroke 1999;30:993-6.
5. Tsai AG, Vandegriff KD, Intaglietta M, Winslow RM. Targeted O2 delivery by low-P50 hemoglobin: a new basis for O2 therapeutics. Am J Physiol 2003;285:H1411-9.
6. Sutherland GR, Farrar JK, Peerless SJ. The effect of Fluosol on oxygen availability in focal cerebral ischemia. Stroke 1984;15:829-35.
7. Cole DJ, Schell RM, Drummond JC. Diaspirin crosslinked hemoglobin (DCLHb): the effect of hemodilution during focal cerebral ischemia in rats. Artif Cells Blood Substit Immobil Biotechnol 1994;22:813-18.
8. Powanda DD, Chang TM. Cross-linked polyhemoglobin-superoxide dismutase-catalase supplies oxygen without causing blood-brain barrier disruption or brain edema in a rat model of transient global brain ischemia-reperfusion. Artif Cells Blood Substit Immobil Biotechnol 2002;30:23-37.
9. Rebel A, Ulatowski JA, Joung K, Bucci E, Traystman RJ, Koehler RC. Regional cerebral blood flow in cats with cross-linked hemoglobin transfusion during focal cerebral ischemia. Am J Physiol 2002;282:H832-41.
10. Bobofchak KM, Mito T, Texel SJ, Belelli A, Nemoto M, Traystman RJ, Koehler RC, Brinigar WS, Fronticelli C. A recombinant polymeric hemoglobin with conformational, functional, and physiological characteristics of an in vivo O2 transporter. Am J Physiol 2003;285:H549-61.
11. Oda T, Nakajima Y, Kimura T, Ogata Y, Fujise Y. Hemodilution with liposome-encapsulated low-oxygen-affinity hemoglobin facilitates rapid recovery from ischemic acidosis after cerebral ischemia in rats. J Artif Organs 2004;7:101-6.

12. Faithfull NS, Fennema M, Erdmann W. Protection against myocardial ischaemia by prior haemodilution with fluorocarbon emulsions. Br J Anaesth 1988;60:773-78.
13. Premaratne S, Harada RN, Chun P, Suehiro A, McNamara JJ. Effect of perfluorocarbon exchange transfusion on reducing myocardial infarct size in a primate model of ischemia-reperfusion injury: a prospective, randomized study. Surgery 1995;117:670-76.
14. George I, Yi GH, Schulman AR, Morrow BT, Cheng Y, Gu A, Zhang G, Oz MC, Burkhoff D, Wang J. A polymerized bovine hemoglobin oxygen carrier preserves regional myocardial function and reduces infarct size after acute myocardial ischemia. Am J Physiol 2006;291:H1126-37.
15. Asanuma H, Nakai K, Sanada S, Minamino T, Takashima S, Ogita H, Fujita M, Hirata A, Wakeno M, Takahama H, Kim J, Asakura M, Sakuma I, Kitabatake A, Hori M, Komamura K, Kitakaze M. S-nitrosylated and pegylated hemoglobin, a newly developed artificial oxygen carrier, exerts cardioprotection against ischemic hearts. J Mol Cell Cardiol 2007; Epub.
16. Chowdary RP, Berkower AS, Moss ML, Hugo NE. Fluorocarbon enhancement of skin flap survival in rats. Plast Reconstr Surg 1987;79:98-101.
17. Altemeier WA, Sinclair SE. Hyperoxia in the intensive care unit: why more is not always better. Curr Opin Crit Care 2007;13:73-8.
18. Erni D, Sakai H, Banic A, Tschopp HM, Intaglietta M. Quantitative assessment of microhemodynamics in ischemic skin flap tissue by intravital microscopy. Ann Plast Surg 1999;43:405-15.
19. Erni D, Sakai H, Tsai AG, Banic A, Sigurdsson GH, Intaglietta M. Haemodynamics and oxygen tension in the microcirculation of ischaemic skin flaps after neural blockade and haemodilution. Br J Plast Surg 1999;52:565-72.
20. Erni D, Wettstein R, Schramm S, Contaldo C, Sakai H, Takeoka S, Tsuchida E, Leunig M, Banic A. Normovolemic hemodilution with Hb vesicle solution attenuates hypoxia in ischemic hamster flap tissue. Am J Physiol 2003;284:H1702-09.
21. Plock J, Tromp A, Contaldo C, Spanholtz T, Sinovcic D, Sakai H, Tsuchida E, Leunig M, Banic A, Erni D. Hemoglobin vesicles reduce hypoxia-related inflammation in critically ischemic hamster flap tissue. Crit Care Med 2007; Epub.
22. Plock JA, Contaldo C, Sakai H, Tsuchida E, Leunig M, Banic A, Menger MD, Erni D. Is hemoglobin in hemoglobin vesicles infused for isovolemic hemodilution necessary to improve oxygenation in critically ischemic hamster skin? Am J Physiol 2005;289:H2624-31.
23. Sakai H, Takeoka S, Park SI, Kose T, Hamada K, Izumi Y, Yoshizu A, Nishide H, Kobayashi K, Tsuchida E. Surface modification of hemoglobin vesicles with poly (ethyleneglycol) and effects on aggregation, viscosity, and blood flow during 90% exchange transfusion in anesthetized rats. Bioconjug Chem 1997;8:15-22.
24. Sakai H, Hara H, Yuasa M, Tsai AG, Takeoka S, Tsuchida E, Intaglietta M. Molecular dimensions of Hb-based O(2) carriers determine constriction of resistance arteries and hypertension. Am J Physiol 2000;279:H908-H15.
25. Contaldo C, Plock J, Sakai H, Takeoka S, Tsuchida E, Leunig M, Banic A, Erni D. New generation of hemoglobin-based oxygen carriers evaluated for oxygenation of critically ischemic hamster flap tissue. Crit Care Med 2005;33:806-12.
26. Fitzpatrick CM, Savage SA, Kerby JD, Clouse WD, Kashyap VS. Resuscitation with a blood substitute causes vasoconstriction without nitric oxide scavenging in a model of arterial hemorrhage. J Am Coll Surg 2004;199:693-701.
27. Sakai H, Tsai AG, Kerger H, Park SI, Takeoka S, Nishide H, Tsuchida E, Intaglietta M. Subcutaneous microvascular response to hemodilution with a red cell substitute consisting of polyethyleneglycol-modified vesicles encapsulating hemoglobin. J Biomed Mater Res 1998;40:66-78.
28. Sakai H, Tsai AG, Rohlfs RJ, Hara H, Takeoka S, Tsuchida E, Intaglietta M. Microvascular response to hemodilution with Hb vesicles as red blood cell substitutes: influence of O2 affinity. Am J Physiol 1999;276:H552-H62.
29. Sakai H, Masada Y, Horinouchi H, Yamamoto M, Ikeda E, Takeoka S, Kobayashi K, Tsuchida E. Hemoglobin-vesicles suspended in recombinant human serum albumin for resuscitation from hemorrhagic shock in anesthetized rats. Crit Care Med 2004;32:539-45.
30. Contaldo C, Schramm S, Wettstein R, Sakai H, Takeoka S, Tsuchida E, Leunig M, Banic A, Erni D. Improved oxygenation in ischemic hamster flap tissue is correlated with increasing hemodilution with Hb vesicles and their O2 affinity. Am J Physiol 2003;285:H1140-7.
31. Intaglietta M. Microcirculatory basis for the design of artificial blood. Microcirculation 1999;6:247-58.
32. Wettstein R, Tsai AG, Erni D, Winslow RM, Intaglietta M. Resuscitation with polyethylene glycol-modified human hemoglobin improves microcirculatory blood flow and tissue oxygenation after hemorrhagic shock in awake hamsters. Crit Care Med 2003;31:1882-4.
33. Sakai H, Takeoka S, Wettstein R, Tsai AG, Intaglietta M,